Certification of standard reference material 1878b respirable α-quartz

David R. Black,[1,a)] Marcus H. Mendenhall,[1] Pamela S. Whitfield,[2,*] Donald Windover,[1] Albert Henins,[1] James Filliben,[1] and James P. Cline[1]
[1]*National Institute of Standards and Technology, Gaithersburg, Maryland 20899*
[2]*Oak Ridge National Lab, Spallation Neutron Source, PO Box 2008, MS-6475, Oak Ridge, Tennessee 37831*

(Received 23 March 2015; accepted 12 April 2016)

The National Institute of Standards and Technology (NIST) certifies a suite of Standard Reference Materials (SRMs) to address specific aspects of the performance of X-ray powder diffraction instruments. This report describes SRM 1878b, the third generation of this powder diffraction SRM. SRM 1878b is intended for use in the preparation of calibration standards for the quantitative analyses of α-quartz by X-ray powder diffraction in accordance to National Institute for Occupational Safety and Health Analytical Method 7500, or equivalent. A unit of SRM 1878b consists of approximately 5 g of α-quartz powder bottled in an argon atmosphere. It is certified with respect to crystalline phase purity, or amorphous phase content, and lattice parameter. Neutron powder diffraction, both time of flight and constant wavelength, was used to certify the phase purity using SRM 676a as an internal standard. A NIST-built diffractometer, incorporating many advanced design features was used for certification measurements for lattice parameters. © *2016 International Centre for Diffraction Data*. [doi:10.1017/S0885715616000336]

Key words: standard reference material, X-ray diffraction, certification, lattice parameter, diffractometer

I. INTRODUCTION

Environmental or occupational exposure to dispersed powders can pose a health risk if inhaled. Typically, an airborne powder or dust cloud is characterized with respect to its health impact by considering the concentration and size distribution of the constituent particles. Three size regimes are considered (see ISO 7708, 1995): inhalable, thoracic, and respirable. The inhaled fraction is that part, which can pass into the nose and mouth. The thoracic part is that fraction which can penetrate beyond the larynx; and finally, the respirable fraction is that part, which can enter the lungs and penetrate into the unciliated airways where it remains. It is this respirable fraction that poses a health risk, causing silicosis, an irreversible pneumoconiosis. For quartz powder, the Occupational Safety and Health Administration (OSHA) defines the respirable size range as between 10 and about 2 μm. The determination is made from the mass fraction of powder passing a size selector such that no particles with an aerodynamic diameter of 10 μm pass the selector and 90% of particles with a diameter of 2 μm pass through. That actual size selection profile is given in Table Z-3 of U.S. Department of Labor (2015). The measurement of the respirable fraction of any dust sample is made using National Institute for Occupational Safety and Health (NIOSH) Analytical Method 7500 (Eller and Cassinelli, 1994). This method relies on a comparison of X-ray diffraction data from material filtered from the dust to that of a standard material of known phase purity. As noted in the text of this method: "Calibration standards are limited to National Institute of Standards and Technology (NIST) and US Geological Survey (USGS) certified standards of known purity, particle size, and sample-to-sample homogeneity".

Standard Reference Material (SRM) 1878b is designed for this purpose and was certified for phase purity using the experimental design described in Cline *et al.* (2011). It is based on the fact that the diffraction experiment is sensitive only to the mass of the crystalline part of material, and cannot account for the amorphous surface layer that exists in all finely divided powders. A weighing operation on the other hand includes the entire mass. If a known mass of an internal standard of known phase purity is mixed with a known mass of the sample, then the discrepancy between this mass fraction and that determined from the diffraction experiment indicates the amorphous content of the sample. Therefore, to quantify the amorphous content in unknowns requires an accurate balance, and a standard of known phase purity, i.e. NIST SRM 676a (2012), and an accurate diffraction experiment.

II. SAMPLE PREPARATION

The feedstock for SRM 1878b was prepared through a collaborative effort between NIST, NIOSH, Cincinnati, OH, and the USGS, Denver, CO. The material used in the preparation of SRM 1878b consisted of single crystal nodules of Brazilian quartz obtained from Top Gem Minerals, Tucson, AZ (Certain commercial equipment, instruments, or materials are identified in order to adequately specify the experimental procedure. Such identification does not imply recommendation or endorsement by the NIST, nor does it imply that the materials or equipment identified are necessarily the best available for

[a)]Author to whom correspondence should be addressed. Electronic mail: david.black@nist.gov
[*]List of authors has been corrected since original publication. An erratum notice detailing this change was also published (doi:10.1017/S0885715616000580).

the purpose). The USGS performed preliminary processing and comminution. The surface contamination was removed from the nodules by combining 9.1 kg (20 lb) aliquots of the quartz nodules with a mixture of water and quartz-sand in a 20 liters plastic carboy. The carboy was placed on a horizontal mixer and the contents mixed for an hour. At the end of the mixing period the quartz crystals were removed from the carboy, washed with deionized water and placed in a drying oven overnight. This process was repeated until the entire supply of quartz was processed. After washing/drying, the quartz was reduced to an average particle size of 1 cm using a 6 inch jaw crusher. Aliquots (25 kg) of the crushed material were transferred to a ceramic lined ball mill and ground for 18 h using 25.4 mm corundum grinding balls. This reduced the median particle size to approximately 1 mm. The material was then transferred to NIST whereupon it was sent to Hosokawa Micron Powder Systems, Summit, NJ, where it was jet milled to a median particle size of 3.3 μm. The disordered, amorphous surface region of the powder was preferentially dissolved with a wash in hydrofluoric acid. Additional contaminants were removed with a second wash in hydrochloric acid. The powder was then rinsed several times and ignited at 500 °C. These treatments were performed by MV Laboratories, Inc., Frenchtown, NJ. The powder was then bottled under Argon by the NIST Standard Reference Material Program (SRMP).

Approximately 2.5 kg of feedstock powder was supplied to SRMP for riffling into bottles containing the 5 g SRM unit mass, yielding a population of 470 units. Ten bottles were removed during this operation using a stratified random sampling and ten bottles of SRM 676a were pulled from the stocks at SRMP. Twenty samples of a nominal 50:50 mass ratio were prepared as described in Cline *et al.* (2011) using two 1 g samples from each bottle, with the pairings of SRM1878b and SRM676a selected at random. The weighing process had an estimated uncertainty of ± 20 μg in each mass, which in turn leads to an uncertainty in mass measurement that is significantly less than that from the X-ray measurements. Five samples were also prepared for neutron diffraction analysis. These samples consisted of 4 g of material, 1 g from each of two bottles of SRM 1878b and 1 g from each of two bottles of SRM 676a, also paired at random. All samples were homogenized in a mortar and pestle.

III. EXPERIMENTAL

A. Procedure for phase purity measurement

The certification for phase purity was performed using neutron diffraction. Time-of-flight (TOF) data were collected at the POWGEN beam line at the Spallation Neutron Source (SNS), Oak Ridge National Laboratory (ORNL) (Huq *et al.,* 2011) and constant wavelength (CW) data were collected on the HB2a High-Resolution Neutron Powder Diffractometer housed at the High Flux Isotope Reactor (HFIR) at ORNL (Garlea *et al.*, 2010). SRM 676a, Alumina Powder for Quantitative Analysis by the X-ray diffraction, which was certified with respect to amorphous content, was used as the internal standard (SRM 676a 2012, Cline *et al.*, 2011).

For the TOF measurement, approximately 3 g of sample were loaded in 8 mm diameter vanadium cans for data collection with center wavelengths of 0.106 6 and 0.265 5 nm at 300 °K. This resulted in diffraction patterns with *d*-spacing between 0.03 and 0.62 nm. For the CW neutron measurement, samples were contained in 6.0 mm diameter by 50 mm long vanadium cans. Data were collected at a wavelength of 0.153 66 nm, which was selected using the [115] reflection from a vertically focused Ge monochromator with collimation of 0.003 3° (12 arc seconds) before the monochromator, 0.005 8° (21 arc seconds) before the sample, and 0.003 3° (12 arc seconds) before the detectors, for a *d*-spacing range of 0.05–0.48 nm. The run time was 2 h and the sample order was randomized on an informal basis.

B. Measurement of lattice parameters and verification of homogeneity

X-ray powder diffraction data were collected on a NIST-built diffractometer that includes several advanced design features. A full discussion of this machine, its alignment and calibration can be found in Cline *et al.* (2015). The optical layout is that of a conventional divergent-beam diffractometer of Bragg–Brentano geometry, equipped with a Johansson incident beam monochromator. Linkage to the International System of Units (SI) (The International System of Units, 2006) is established via the emission spectrum of Cu$K\alpha$ radiation employed as the basis for constructing the diffraction profiles via the fundamental parameters approach (FPA) (Cheary and Coelho, 1992) method of data analysis. The models for the geometric component of the profiles included source and receiving slit width, flat specimen error, and axial divergence. Rigorous analyses of data from this divergent beam diffractometer require knowledge of both the diffraction angle and the effective source–sample–detector distance. Therefore, additional models must be included in the data analyses to account for the factors that affect the distances critical in the use of this geometry. Data were analyzed in the context of both type A uncertainties, assigned by statistical analysis, and type B uncertainties, based on knowledge of the nature of errors in the measurements, to result in the establishment of robust uncertainties for the certified values (Taylor and Kuyatt, 1994; Guide to the Expression of Uncertainty in Measurement, 2008).

The 1.5 kW copper tube of fine focus geometry was operated at a power of 1.2 kW. The variable divergence incident slit was set to 0.9° with a 0.2 mm (0.05°) receiving slit. Data were collected with a step width of 0.01° 2θ and a count time of 5 s per point to result in a scan time of roughly 24 h. Samples were spun about their surface normal at 0.5 Hz during data collection. The machine was located within a temperature-controlled laboratory space where the nominal short-range control of temperature was ± 0.1 °C. The temperature and humidity were recorded during data collection using Veriteq SP 2000 monitors stated to be accurate to ± 0.15 °C. The X-ray source was allowed to equilibrate at operating conditions for at least 1 h prior to recording any certification data. The performance of the machine was qualified with the use of NIST SRM 660b Lanthanum Hexaboride Powder Line Position and Line Shape Standard for Powder Diffraction (SRM 660b, 2010; Black *et al.*, 2011) and SRM 676a using procedures discussed by Cline *et al.* (2015).

IV. DATA ANALYSIS

A. Neutron data

The TOF and CW data were analyzed with the Rietveld method utilizing the software General Structure Analysis

https://doi.org/10.1017/S0885715616000336 Published online by Cambridge University Press

System (GSAS) (Larson and Von Dreele, 2003). This was done with two refinements, one for each experimental method, which included the five sets of data collected for that particular method. The refined parameters common to both analyses included: scale factors, lattice parameters of the SRM 1878b, atomic positional, and thermal parameters. For the TOF data, calibration runs using SRM 660b were used to determine the terms of the GSAS TOF profile function-3 (Von Dreele *et al.,* 1982), and values for DIFC, DIFA, and zero. With the analysis of the SRM 1878b/676a mixtures, only the terms pertaining to Lorentzian size broadening were refined and they were constrained with respect to histogram and phase. Given that the lattice parameters of SRM 676a were fixed at certified values, the diffractometer constants DIFA and zero were refined. The TOF refinement also included four terms of a shifted Chebyshev background function. The CW data were analyzed using the GSAS profile function type 3 (Thompson *et al.,* 1987). Refined terms included GU, GV, GW, LZ, LY, and SL; all but LX and LY were constrained globally; the LX and LY terms were constrained by phase. The Finger model (Finger *et al.,* 1994) was used to account for profile asymmetry; however, the S/L and H/l terms are highly correlated, only one term, SL, was refined while the other was fixed at a value nominally identical to the first. Also, given that the lattice parameters of the SRM 676a phase were fixed, the wavelength and zero values were refined. The CW refinement included five terms of a shifted Chebyshev background function.

The scale factors in GSAS are proportional to the numbers of unit cells from each phase, which allows quantitative data to be obtained with the following relation:

$$\frac{X_\alpha}{\sum X_\mathrm{p}} = \frac{S_\alpha Z_\alpha w_\alpha}{\sum S_\mathrm{p} Z_\mathrm{p} w_\mathrm{p}}, \tag{1}$$

where X_α is the mass fraction of phase α, S_p are the scale factors, w_p are the molecular weights, and Z_p are the number of formula weights per unit cell, and the summations are carried out over the various phases within the mixture. Use of this equation allows for "standardless" analysis only if one can assume that ΣX_p is 1; i.e. there is no amorphous content and all of the crystalline phases are included in the analysis. Under these conditions, there are an equal number of unknowns and equations. However, if there is amorphous component then ΣX_p is another unknown and:

$$\sum X_\mathrm{p} + X_\mathrm{amor} = 1. \tag{2}$$

Analysis for amorphous content requires the addition of a standard of known purity. We now consider that both the standard and the unknown contain both crystalline and amorphous fractions:

$$\sum X_\mathrm{u} = \sum X_\mathrm{u-cry} + \sum X_\mathrm{u-amor}, \tag{3}$$

and

$$X_\mathrm{stn} = X_\mathrm{stn-cry} + X_\mathrm{stn-amor}. \tag{4}$$

The fraction of standard added, X_stn, provides another equation of type 1 with the only unknown being ΣX_p:

$$\frac{X_\mathrm{stn-cry}}{\sum X_\mathrm{p}} = \frac{S_\mathrm{stn-cry} Z_\mathrm{stn-cry} w_\mathrm{stn-cry}}{\sum S_\mathrm{p} Z_\mathrm{p} w_\mathrm{p}}. \tag{5}$$

In this case,

$$\sum X_\mathrm{p} = \sum X_\mathrm{u-cry} + X_\mathrm{stn-cry}. \tag{6}$$

Therefore,

$$\frac{X_\mathrm{stn-cry}}{\sum X_\mathrm{u-cry} + X_\mathrm{stn-cry}} = \frac{S_\mathrm{stn-cry} Z_\mathrm{stn-cry} w_\mathrm{stn-cry}}{\sum \mathrm{S_p Z_p w_p}} \tag{7}$$

and

$$\left(\sum X_\mathrm{u-cry} + \sum X_\mathrm{u-amor}\right) + (X_\mathrm{stn-cry} + X_\mathrm{stn-amor}) = 1. \tag{8}$$

The terms in Eq. (7) refer only to the crystalline components of the mixture and, as such, the unknown(s) in Eq. (8) are determined through the diffraction experiment. The terms within the parentheses of Eq. (8) are the mass fractions of the unknown and standard, which are known from the weighing operation when the specimens were prepared. The right-hand side of Eq. (5) is the mass fraction of the standard determined from the Rietveld analysis, $\mathrm{MF_{stn}}$, and allows for the determination of $\Sigma X_\mathrm{u\text{-}cry}$. Equation (6) is then used to determine $X_\mathrm{u\text{-}amor}$. Solving Eq. (5) for $\Sigma X_\mathrm{u\text{-}cry}$ and making this substitution into Eq. (6) we get:

$$\sum X_\mathrm{u-cry} = \frac{X_\mathrm{stn-cry}}{\mathrm{MF_{stn}}} - X_\mathrm{stn-cry} \tag{9}$$

and

$$\sum X_\mathrm{u-amor} = 1 - \left(\frac{X_\mathrm{stn-cry}}{\mathrm{MF_{stn}}} - X_\mathrm{stn-cry}\right) - X_\mathrm{stn-cry} - X_\mathrm{stn-amor}. \tag{10}$$

The value of $\Sigma X_\mathrm{u\text{-}amor}$ must be normalized with respect to ΣX_u to yield mass fraction of amorphous material in the unknown. The refined mass fractions of SRM 676a determined through these analyses are shown in Figure 1. The certified value for crystalline phase purity of the material expressed as a mass

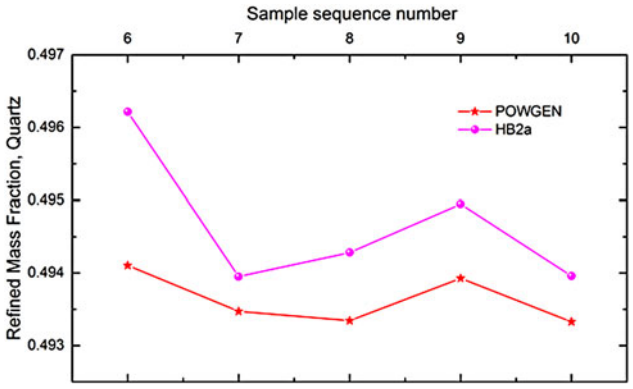

Figure 1. (Color online) The mass fractions of quartz obtained from Rietveld refinements of the neutron powder diffraction data from POWGEN (TOF) and HB2a (CW).

https://doi.org/10.1017/S0885715616000336 Published online by Cambridge University Press

TABLE I. The refined mass fractions and lattice parameters derived from analyses of the X-ray diffraction data.

Bottle number	Refined mass fraction quartz	Lattice parameter a (nm)	Lattice parameter c (nm)
313b	0.507 625 55	0.491 405 5	0.540 557 0
183b	0.513 146 52	0.491 407 6	0.540 551 4
256a	0.506 987 85	0.491 410 2	0.540 561 6
424b	0.511 88	0.491 406 6	0.540 549 1
66b	0.512 558 76	0.491 407 0	0.540 554 2
349b	0.512 090 25	0.491 407 0	0.540 554 6
343b	0.511 384 44	0.491 407 3	0.540 556 4
1b	0.510 170 4	0.491 405 4	0.540 553 1
313a	0.510 006 93	0.491 402 1	0.540 551 7
424a	0.509 777 89	0.491 405 8	0.540 549 2
256b	0.516 399 84	0.491 404 6	0.540 557 9
349a	0.511 035 29	0.491 407 9	0.540 552 8
183a	0.508 075 77	0.491 402 5	0.540 553 5
393a	0.510 372 05	0.491 411 5	0.540 559 1
488a	0.510 340 58	0.491 404 5	0.540 553 0
66a	0.508 505 5	0.491 406 9	0.540 550 0
122a	0.509 379 76	0.491 406 9	0.540 555 0
488b	0.506 434 02	0.491 407 2	0.540 552 6
1a	0.501 280 79	0.491 402 7	0.540 553 7
122b	0.510 924 37	0.491 408 1	0.540 562 2

fraction is 96.56 ± 0.40%. The interval defined by the certified value and its uncertainty represents an expanded uncertainty using the coverage factor, $k = 2$, in the absence of systematic error, were calculated according to the method described in JCGM 100 (2008).

B. X-ray data

The X-ray diffraction certification data were analyzed using the FPA method with a Rietveld refinement as implemented in TOPAS (2009) and a NIST Python-based code that replicates the FPA method in the computation of X-ray powder diffraction line profiles (Mendenhall *et al.,* 2015). The analysis used energies of the Cu$K\alpha_1$ emission spectrum as characterized by Hölzer *et al.* (1997). The refined parameters included the scale factors, Chebyshev polynomial terms for modeling of the background, the lattice parameters, specimen displacement and attenuation terms, structural parameters, terms for Lorentzian size, and strain broadening, a Gaussian strain profile was also refined for the quartz of SRM 1878b. FPA analysis of SRM 660b was performed as part of the calibration of the instrument and included the full range of parameters pertinent to the IPF (Cline *et al.,* 2015). With the analysis of data from SRM 660b, the refined Soller slit value with the "full" axial divergence model (Cheary and Coelho, 1998a,b), was 3.2°. However, non-physical values for the incident slit size, 1.1 vs. 0.9°, and unrealistically low sample attenuation values were obtained. This is indicative of a problem with the model and is under investigation. With analyses of SRM 1878b, the Soller slit values were set at 3.2° and the incident slit size was fixed at 1.1°. The refined mass fraction of quartz, and the a and c lattice parameters obtained from the 20 specimens of SRM 1878b are listed in Table I. The statistical, type A, evaluation of the lattice parameters resulted in estimates of $a = 0.491\,406\,37$ and $c = 0.540\,554\,41$ nm with $k = 2$ expanded uncertainties of 0.000 001 06 and 0.000 001 65 nm for a and c, respectively. However, the components of uncertainty that were evaluated by type B methods must also be taken into account.

C. Assessment of type B errors in lattice parameters

In order to assess the systematic, type B, uncertainties in the lattice parameter values, the difference between lattice parameters obtained with an FPA Rietveld analyses of SRM 676a and those obtained with a profile analysis were plotted (Figure 2). The models used in the FPA profile analysis were constrained over the entire range as per the Rietveld method, but for the profile analysis, profile positions were allowed to refine independently with a lattice parameter being computed for each profile position. If the FPA model were operating in a "perfect" manner, the data of Figure 2 would constitute a horizontal line as there would be no difference in the Rietveld vs. profile values. Overall, we judge a type B error of ± 20 fm to be appropriate. Therefore, the certified lattice parameters are $a = 0.491\,406 \pm 0.000\,020$ nm and $c = 0.540\,554 \pm 0.000\,020$ nm. The certified lattice parameters were adjusted using the coefficient of thermal expansion values found in Kosinski *et al.* (1992) to values at 22.5 °C.

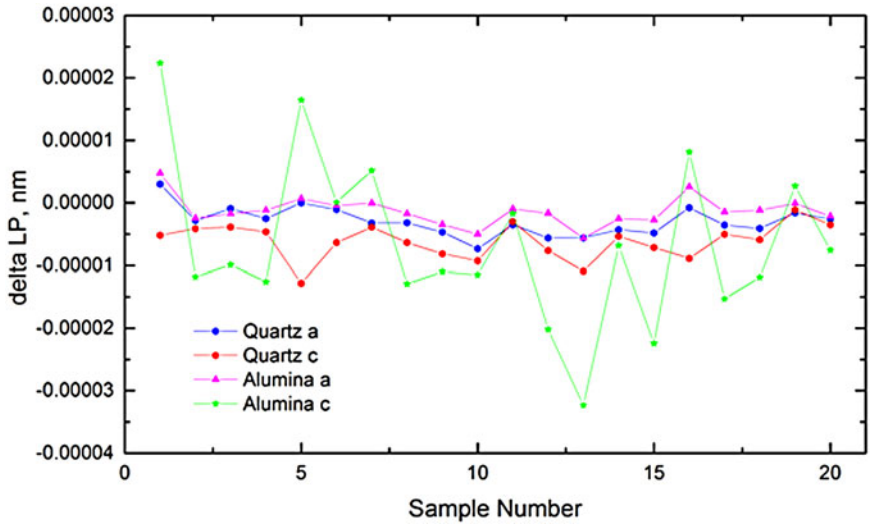

Figure 2. (Color online) The difference in lattice parameter values for SRM 676a obtained from a FPA Rietveld refinement using the NIST Python-based FPA code and those from a profile-fitting analysis of X-ray powder diffraction data.

https://doi.org/10.1017/S0885715616000336 Published online by Cambridge University Press

V. CONCLUSION

The phase purity and lattice parameters of α-quartz have been certified using neutron and X-ray powder diffraction. TOF and CW neutron diffraction from nominal 50:50 mixtures of SRM 1878b and SRM 676a provide for the certification of phase purity. The phase purity is certified to be 96.56 ± 0.40%. X-ray diffraction data from similar 50:50 mixtures, using a NIST built diffractometer, provided for the certification of the lattice parameters. The certified lattice parameters are $a = 0.491\,406 \pm 0.000\,020$ nm and $c = 0.540\,554 \pm 0.000\,020$ nm at 22.5 °C. These values incorporate an expanded type B uncertainty assigned based on a comparison of two different analysis methodologies.

Black, D., Windover, D., Henins, A., Filliben, J. J., and Cline, J. P. (**2011**). "Certification of standard reference material 660B," Powder Diffr. **26** (2), 155–158.

Cheary, R. W., Coelho, A. A. (**1992**) "A fundamental parameters approach to X-ray line-profile fitting," J. Appl. Cryst., **25**, 109–121.

Cheary, R. W., Coelho, A. A. (**1998a**) "Axial divergence in a conventional X-ray powder diffractometer II, implementation and comparison with experiment," J. Appl. Crystallogr., **31**, 862–868.

Cheary, R. W. and Coelho, A. A. (**1998b**). "Axial divergence in a conventional X-ray powder diffractometer I. theoretical foundations," J. Appl. Crystallogr., **31**, 851–861.

Cline, J. P., Mendenhall, M. H., Black, D., Windover, D., and Henins, A. (**2015**). "The optics, alignment and calibration of laboratory X-ray powder diffraction equipment with the use of NIST standard reference materials," J. Res. NIST **120**, 173–222.

Cline, J. P., Von Dreele, R. B., Winburn, R., Stephens, P. W., and Filliben, J. J. (**2011**). "Addressing the amorphous content issue in quantitative phase analysis, the certification of NIST standard reference material 676a," Acta Crystallogr. **A67**, 357–367.

Eller, P. and Cassinelli, M., Eds. (**1994**). *NIOSH Manual of Analytical Methods (NMAM)*, 4th ed., (DHHS (NIOSH) Publication No. 94-113).

Finger, L. W., Cox, D. E., and Jephcoat, A. P. (**1994**). "A correction for powder diffraction peak asymmetry due to axial divergence," J. Appl. Crystallogr. **27**, 892–900.

Garlea, V. O., Chakoumakos, B. C., Moore, S. A., Taylor, G. B., Chae, T., Maples, R. G., Riedel, R. A., Lynn, G. W., and Selby, D. L. (**2010**). "The high-resolution powder diffractometer at the high flux isotope reactor," Appl. Phys. A **99**(3), 531–535.

Guide to the Expression of Uncertainty in Measurement (GUM). (**2008**). Joint Committee for Guides in Metrology (JCGM/WG 1). Available at: http://www.bipm.org/en/publications/guides/gum.html

Hölzer, G., Fritsch, M., Deutsch, M., Härtwig, J., and Förster, E. (**1997**). "$K\alpha_{1,2}$ and $K\beta_{1,3}$ X-ray emission lines of the 3d transition metals," Phys. Rev. A **56**(6), 4554–4568.

Huq, A., Hodges, J. P., Gourdon, O., and Heroux, L. (**2011**). "Powgen: a third-generation high-resolution high-throughput powder diffraction instrument at the spallation neutron source," Z. Kristallogr. Proc. **1**, 127–135, DOI 10.1524/zkpr.2011.0019.

ISO 7708 (**1995**). Air Quality – Particle Size Fraction Definitions for Health-related Sampling ISO Standard 7708. Available at: ftp://ftp.cdc.gov/pub/Documents/OEL/02.%20Kuempel/References/ISO_1995-Report%20No%207708.pdf (accessed June 2015).

JCGM 100 (**2008**). Guide to the Expression of Uncertainty in Measurement; (GUM 1995 with Minor Corrections), Joint Committee for Guides in Metrology (JCGM). Available at: http://www.bipm.org/utils/common/documents/jcgm/JCGM_100_2008_E.pdf (accessed June 2015).

Kosinski, J. A., Gualtieri, J. G., and Ballato, A. (**1992**). "Thermoelastic coefficients of alpha quartz," IEEE Trans. Ultrason. Ferroelectr. Freq. Control **39**(4), 502–7.

Larson, A. C. and Von Dreele, R. B. (**2003**). *General Structure Analysis System (GSAS)*, (Report LAUR 86–748). (Los Alamos National Laboratory, Los Alamos, NM).

Mendenhall, M. H., Mullen, K., and Cline, J. P. (**2015**). "An implementation of the fundamental parameters approach for analysis of X-ray powder diffraction line profiles," J. Res. NIST **120**, 223–251.

SRM 660b (**2010**). *Line Position and Line Shape Standard for Powder Diffraction* (National Institute of Standards and Technology, U.S. Department of Commerce, Gaithersburg, MD).

SRM 676a (**2012**). *Alumina Powder for Quantitative Analysis by X-ray Diffraction* (National Institute of Standards and Technology, U.S. Department of Commerce, Gaithersburg, MD.

Taylor, B. N. and Kuyatt, C. E. (**1994**). *Guidelines for Evaluating and Expressing the Uncertainty of NIST Measurement Results, NIST Technical Note 1297*, (U.S. Government Printing Office, Washington, DC). http://physics.nist.gov/Pubs/

The International System of Units (SI) (**2006**). (8th ed.), ISBN 92-822-2213-6. http://www.bipm.org/utils/common/pdf/si_brochure_8_en.pdf, Bureau International des Poids et Mesures, Sèvres, France.

Thompson, P., Cox, D. E., and Hastings, J. B. (**1987**). "Rietveld refinement of Debye–Scherrer synchrotron X-ray data from Al_2O_3," J. Appl. Crystallogr. **20**, 79–83.

U.S. Department of Labor (**2015**). Office of the Federal Register, and Government Printing Office. TABLE Z-3 Mineral Dusts from e-CFR Title 29, Subtitle B, Chapter XVII, Part 1910, Subpart Z, 1910.1000. Available at: http://www.ecfr.gov/. (accessed 10 Jun 2015).

Von Dreele, R. B., Jorgensen, J. D., and Windsor, C. G. (**1982**). "Rietveld refinement with spallation neutron powder diffraction data," J. Appl. Crystallogr. **15**, 581–589.

https://doi.org/10.1017/S0885715616000336 Published online by Cambridge University Press